

Carbosilane Dendrimers with Perfluoroalkyl End Groups. Core–Shell Macromolecules with Generation-Dependent Order

Klaus Lorenz, Holger Frey,* Bernd Stühn,[†] and Rolf Mülhaupt

Institut für Makromolekulare Chemie/Freiburger Materialforschungszentrum
FMF der Albert-Ludwigs-Universität Freiburg, Stefan-Meier-Strasse 21/31,
D-79104 Freiburg, Germany

Received February 28, 1997; Revised Manuscript Received July 10, 1997[®]

ABSTRACT: A series of carbosilane dendrimer generations, G0 to G3, with 4, 12, 36, and 108 end groups, respectively, has been functionalized with perfluorohexyl (C_6F_{13} –) groups on the surface. Quantitative perfluoroalkylation of the dendrimer surface was achieved via free radical addition of 3,3,4,4,5,5,6,6,7,7,8,8,8-tridecafluoro-*n*-octyl mercaptan. Quantitative perfluoroalkylation of the dendrimers was demonstrated by NMR and SEC. The thermal properties of the dendrimers with core–shell structure were investigated by DSC, polarizing microscopy, and WAXS. Whereas G0 was obtained as a crystalline material that did not show the formation of mesophases, G1 (12 end groups) exhibited the formation of a highly ordered smectic mesophase between -15 and -30 °C. In contrast, G2 and G3 did not form mesophases; however, a transition to a most probably hexagonally ordered array of columns could be observed. The generation-dependent thermal behavior is ascribed to the increasingly dense packing of perfluorohexyl groups on the dendrimer surface.

Introduction

Dendrimers with core–shell structure are intriguing macromolecules due to their potential usefulness as unimolecular micelles,¹ which may act as solubilizers and hosts for organic guest molecules. Such dendrimers possess potential in phase transfer catalysis or might serve as recyclable extracting agents.² Furthermore, use of dendritic structures of this type for the purpose of controlled drug release is discussed.³ Recent research efforts in the area of dendritic structures are also directed toward the combination of branched topologies and liquid crystals, i.e., the synthesis of highly branched macromolecules with mesogenic units and supramolecular structures of such systems. For example, hyperbranched polymers based on rigid aromatic or mesogenic branching units show lyotropic⁴ or thermotropic cholesteric⁵ and nematic⁶ mesophases depending on the mesogenic unit attached. Perfect dendrons and dendrimers with mesogenic branching units were found to exhibit cybotactic nematic and smectic mesophases.⁷

We have recently employed carbosilane dendrimers for the attachment of mesogenic units, such as cyanobiphenyl⁸ and cholesteryl⁹ groups. Such flexible dendrimers with mesogenic end groups are unable to crystallize due to their highly branched structure; however, the materials exhibit thermotropic liquid crystalline behavior, if the size of the molecule and the spacer length between mesogenic unit and dendritic scaffold are appropriately chosen. Based on these results, we were interested in the effect of perfluoroalkyl end groups that are immiscible with the core of the carbosilane dendrimers. Linear amphiphiles that consist of hydrocarbon and perfluorinated segments with at least six CF_2 groups show liquid crystalline (LC) phases that originate from the immiscibility of the hydrocarbon and the perfluoroalkyl part of the compounds but have also been explained by the relative stiffness of the perfluorinated segments compared with the highly flexible hydrocarbon part.¹⁰ In contrast,

triblock molecules of the structure $\text{F}(\text{CF}_2)_{12}(\text{CH}_2)_m$ ($\text{CF}_2)_{12}\text{F}$ exhibit only melting transitions from the solid state to the melt.¹¹ The solid–solid phase transitions and the solution behavior of amphiphiles with perfluoroalkyl segments have been reviewed recently.¹² Microblock copolymers consisting of alternating hydrocarbon and perfluorinated segments have been synthesized by Griffin et al.¹³ and show smectic mesophases.¹⁴ Perfluorinated side chains attached to tapered molecules are found to introduce their aggregation to columnar mesophases or to widen the stability range of these LC phases.¹⁵ Layerlike ordering of side groups can be induced by perfluorinated alkyl chains due to their phase-segregating power.¹⁶ Furthermore, highly hydrophobic perfluorinated dendritic wedges have been attached to poly(ethylene oxide), leading to polymers that were able to solubilize water-insoluble dyes due to micelle formation.¹⁷

In spite of these extensive studies of linear structures combining perfluoroalkyl segments and hydrocarbon chains, no dendrimers with perfluoroalkyl groups on the surface have been reported yet. Furthermore, the combination of a perfect dendrimer topology and perfluorinated groups has not been studied with respect to supramolecular order yet. In this paper, we present the synthesis and characterization of a series of four carbosilane dendrimers (G0-(RF6)₄, G1-(RF6)₁₂, G2-(RF6)₃₆, and G3-(RF6)₁₀₈) bearing 4, 12, 36, and 108 C_6F_{13} (RF6) end groups, respectively, as well as the generation-dependent thermal behavior of such core–shell type dendrimers.

Experimental Section

Materials. 3,3,4,4,5,5,6,6,7,7,8,8,8-Tridecafluoro-*n*-octyl mercaptan was received from Ciba and distilled in vacuo before use. The carbosilane dendrimers (G0, G1, G2, and G3) were prepared as described previously.^{18b} 2,2'-Azobis(isobutyronitrile) (AIBN) was purchased from Fluka. Heptane (p.a. grade) was purchased from Roth and used as received. All solvents and reagents for workup procedures were used as received.

General. All glassware was dried carefully before use. Dendrimer solutions were degassed four times before adding the radical initiator according to the

[†] Fakultät für Physik, Universität Freiburg, Hermann-Herder-Str. 3, D-79104 Freiburg, Germany.

[®] Abstract published in *Advance ACS Abstracts*, October 1, 1997.

following procedure: The reaction solution was frozen in liquid N₂ and then evacuated (20 mbar). The flask was sealed and warmed to ambient temperature. After warming, the flask was refilled with Ar.

Methods. NMR. Solution ¹H-NMR spectra were recorded on a 300 MHz (Bruker) spectrometer in CDCl₃ (G0-(RF6)₄, G1-(RF6)₁₂), C₆D₆/C₆F₆ 1:1 (G2-(RF6)₃₆) and in perfluorohexane saturated with perdeuteriooctane (G3-(RF6)₁₀₈). ¹H chemical shifts are referenced to signals of the solvents used.

Differential Scanning Calorimetry (DSC). A Perkin-Elmer DSC 7 was used to monitor phase transitions and *T_g*'s. Phase transitions were generally determined at a scan rate of 3 °C/min (heating). All *T_g*'s were determined at a scan rate of 20 °C/min (heating). Sample weights were typically chosen between 7 and 10 mg. The instrument was calibrated with high-purity samples of indium and cyclohexane.

Size Exclusion Chromatography (SEC). A combination of PL columns (Polymer Laboratories), 10⁵, 10⁴, 10³, and 100 nm, was employed. CHCl₃ was used as solvent. All data are referenced to narrow polystyrene standards.

Polarizing Optical Microscopy (POM). The optical microscope used was a Leitz Ortholux II Pol-BK equipped with a Mettler FP82 hotstage. The polarizing light photomicrograph shown in Figure 4 was obtained after annealing the sample at -17 °C for 1 h.

WAXS. The WAXS profiles were obtained with a Siemens D500 diffractometer, which has been modified to operate under computer control. The scans were performed in the θ -2 θ mode, rotating both the sample and the detector. The X-ray beam from a sealed Cu anode in a sealed tube was scattered in reflection geometry and analyzed with a secondary monochromator and a scintillation counter. The selected wavelength is $\lambda = 1.541$ Å. The sample was contained in an evacuated chamber (Paar, Graz, Austria), which allowed heating and cooling with a temperature stability better than 0.5 K.

G1-(RF6)₁₂ was annealed at -24 °C for 30 min and subsequently cooled rapidly to -50 °C (below *T_g*) in order to avoid leaking out of the liquid while slanting the sample holder. The sample holder containing the liquid G2-(RF6)₃₆ at ambient temperature was wrapped with a thin aluminum foil. Samples of G2-(RF6)₃₆ and G3-(RF6)₁₀₈ were not annealed at the respective temperatures. The measurements were performed in vacuo.

IR. A Perkin-Elmer infrared spectrophotometer 1330 was used. The samples were prepared as thin films between KBr single crystals.

Synthesis. G0-(RF6)₄. A 50 mL two-necked flask was charged with 1.1 g (5.7 mmol) of tetraallylsilane and 10.83 g (28.6 mmol) of 3,3,4,4,5,5,6,6,7,7,8,8,8-tridecafluoro-*n*-octyl mercaptan. After the solution had been degassed four times, 47 mg (0.28 mmol) of AIBN was added under Ar. The reaction mixture was stirred at 80 °C for 12 h. After cooling to ambient temperature, diethyl ether was added. The ether solution of the crude reaction product was washed several times with concentrated aqueous NaOH solution and eventually with water. The organic layer was then dried with MgSO₄, filtered off, and concentrated. After removal of the ether, a small amount of pentane was added. Ethanol was added slowly to the stirred pentane solution until a slight turbidity occurred. The flask was kept at 4 °C overnight and 5.8 g (59%) of white crystals was filtered off from the cold solution. ¹H-NMR (CDCl₃, ppm, "RF"

designates -(CF₂)₅CF₃): 0.6 (t, 8 H, SiCH₂), 1.5 (m, 8H, SiCH₂CH₂CH₂), 2.3 (m, 8 H, RFCH₂CH₂S), 2.5 (t, 8 H, SiCH₂CH₂CH₂S), 2.7 (t, 8 H, RFCH₂CH₂S). Mp: 23 °C.

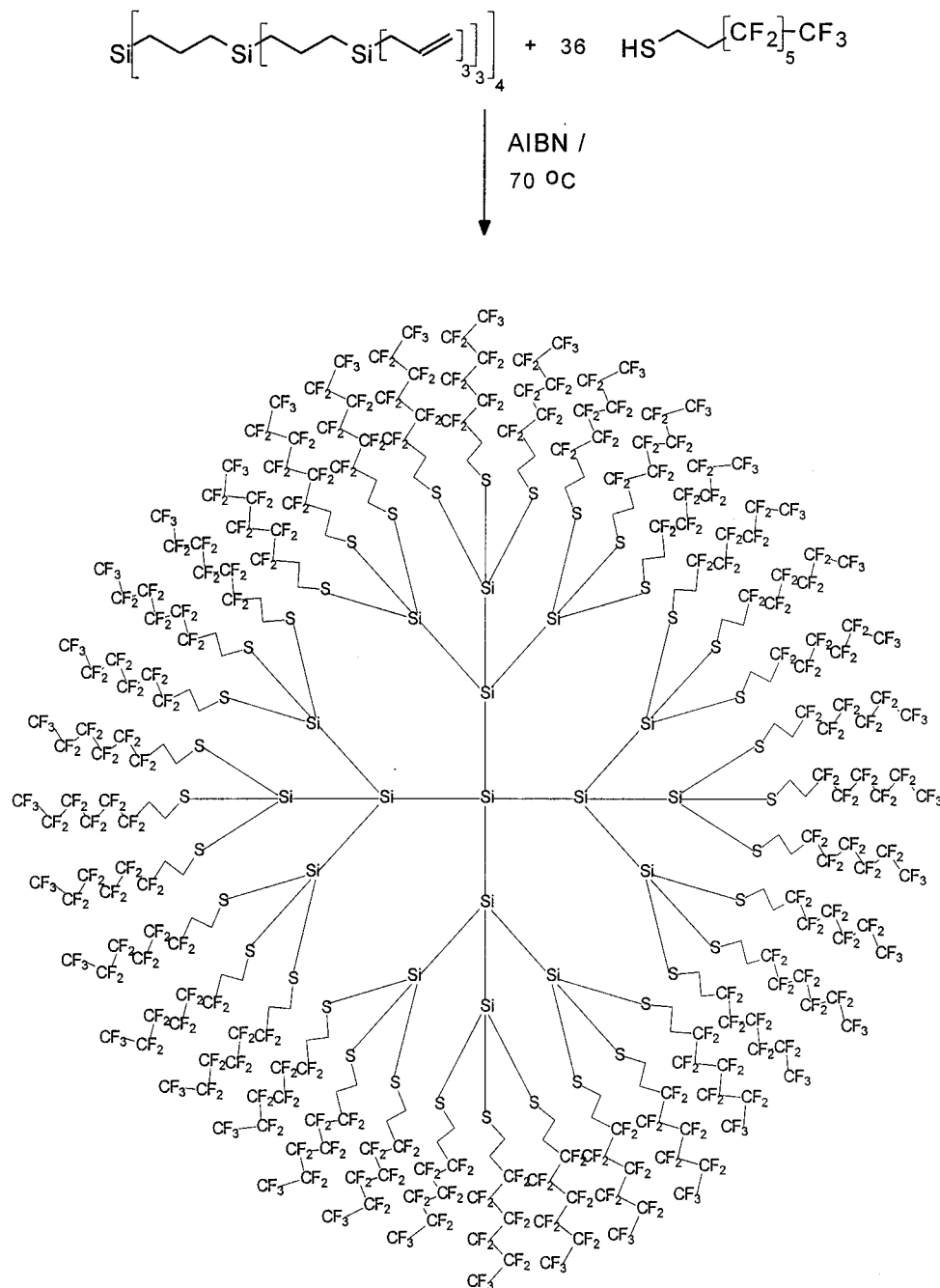
G1-(RF6)₁₂. A 50 mL two-necked flask was charged with 0.3 g (0.3742 mmol) of G1 and 2.689 g (7.073 mmol) of 3,3,4,4,5,5,6,6,7,7,8,8,8-tridecafluoro-*n*-octyl mercaptan. After the solution had been degassed four times, 23.23 mg (0.142 mmol) of AIBN was added under Ar. The reaction mixture was stirred at 80 °C for 20 h. The reaction product was precipitated six times from a petroleum ether solution by adding ethanol. Yield: 1.49 g (74%). ¹H-NMR (CDCl₃, ppm, "RF" designates -(CF₂)₅CF₃): 0.6 (m, 40 H, (SiCH₂CH₂CH₂SiCH₂), 1.3 (m, 8 H, SiCH₂CH₂CH₂Si), 1.6 (m, 24 H, (SiCH₂CH₂CH₂S), 2.3 (m, 24 H, (SCH₂CH₂RF), 2.5 (t, 24 H, SiCH₂CH₂CH₂S), 2.7 (SCH₂CH₂RF).

G2-(RF6)₃₆. A 50 mL two-necked flask was charged with 557 mg (0.212 mmol) of G2 and 5.64 g (14.83 mmol) of 3,3,4,4,5,5,6,6,7,7,8,8,8-tridecafluoro-*n*-octyl mercaptan. *n*-Heptane was added dropwise until the reaction mixture became clear. After the solution had been degassed four times, 11 mg (0.061 mmol) of AIBN was added under Ar. The flask was kept at 70 °C for 22 h under stirring. Thereafter, 10 mg (0.055 mmol) of AIBN and again 1.5 g of 3,3,4,4,5,5,6,6,7,7,8,8,8-tridecafluoro-*n*-octyl mercaptan were added. The solution was once more thoroughly degassed and subsequently kept at 70 °C for 22 h. After evaporation of the solvent, the product was purified by extracting four times with boiling CHCl₃. Yield: 2.967 g (86%). ¹H-NMR (C₆D₆/C₆F₆ 1:1, ppm, "RF" designates -(CF₂)₅CF₃): 1.1 (overlapped, m, 208 H, SiCH₂CH₂CH₂Si and SiCH₂CH₂CH₂S), 1.8–2 (overlapping, m, 104 H, SiCH₂CH₂CH₂Si and SiCH₂CH₂CH₂S), 2.6 (m, 72 H, SCH₂CH₂RF), 2.9–3.1 (m, 144 H, SiCH₂CH₂CH₂S and SCH₂CH₂RF).

G3-(RF6)₁₀₈. A 50 mL two-necked flask was charged with 0.155 g (0.0191 mmol) of G3 and 1.255 g (3.3012 mmol) of 3,3,4,4,5,5,6,6,7,7,8,8,8-tridecafluoro-*n*-octyl mercaptan. *n*-Heptane was added dropwise until the reaction mixture became clear. After the solution had been degassed four times, 12.5 mg (0.076 mmol) of AIBN was added under Ar. The reaction mixture was stirred at 80 °C for 20 h. Thereafter, 6 mg (0.0365 mmol) of AIBN and eight droplets of 3,3,4,4,5,5,6,6,7,7,8,8,8-tridecafluoro-*n*-octyl mercaptan were added. The solution was once more thoroughly degassed and subsequently heated at 80 °C for 20 h. The solvent was evaporated, and the product was purified by extracting three times with boiling CHCl₃. Before each removal of the solvent, the flask was kept at -16 °C for several hours. Yield: 0.61 g (65%). ¹H-NMR (perfluorohexane saturated with perdeuteriooctane, ppm, "RF" designates -(CF₂)₅CF₃): 1.5–1.8 (overlapping, m, 424 H, SiCH₂CH₂CH₂Si and SiCH₂CH₂CH₂S), 1.5 (shoulder), 2.05 (hydrogen atoms of incompletely deuterated octane), 2.35 and 2.6 (overlapping, m, 320 H, SiCH₂CH₂CH₂Si and SiCH₂CH₂CH₂S), 3.3, 3.6, and 3.7 (overlapped, 864 H, SCH₂CH₂RF, SiCH₂CH₂CH₂S, and SCH₂CH₂RF), 6.5, 6.75, and 6.8 (t, incompletely fluorinated perfluorohexane).

Results and Discussion

(A) Synthesis and Characterization. Synthesis and characterization of the carbosilane dendrimers used for the preparation of the perfluoroalkyl-substituted derivatives have been described elsewhere.¹⁸ Attachment of the perfluorinated alkyl groups to the allylic end groups of the dendrimers was performed via free

Scheme 1. Synthesis and Schematic Representation of G2-(RF6)₃₆

radical addition of 3,3,4,4,5,5,6,6,7,7,8,8,8-tridecafluoro-*n*-octyl mercaptan (HS(CH₂)₂(CF₂)₆F), which affords the corresponding thioether-functionalized end groups. We employed AIBN as a radical source; however, mercaptan addition to carbon–carbon double bonds can also be initiated by photochemical means¹⁹ or by catalytic amounts of 9-BBN.²⁰ In order to achieve complete reaction of all allylic end groups, the fluorinated mercaptan was used in excess (20%–60%). The reaction was monitored by IR and NMR spectroscopy to follow the degree of conversion. The synthesis and structure of a perfluorinated dendrimer of the second generation (G2-(RF6)₃₆) are displayed in Scheme 1.

G0-(RF6)₄ (4 end groups, *M_w*(calc) = 1713.07) and G1-(RF6)₁₂ (12 end groups, *M_w*(calc) = 5363.64) could be synthesized in bulk, i.e., the fluorinated mercaptan was used as solvent, whereas the synthesis of G2-(RF6)₃₆ (36 end groups, *M_w*(calc) = 16315.41) and G3-(RF6)₁₀₈ (108 end groups, *M_w*(calc) = 49170.71) required the addition

of heptane as cosolvent to ensure initial solubility of all components in the reaction medium. Prior to heating to the reaction temperature, the reaction solution had to be degassed in order to avoid formation of disulfides via oxidative coupling of mercaptans. Whereas complete conversion of the allyl end groups was achieved for G0, G1, and G2, under the conditions used, it was not possible to convert all allyl end groups of G3 into the desired thioether functions. This is most probably due to increasing steric congestion on the dendrimer surface, because (i) the cross section of perfluorinated chain segments is larger than that of hydrocarbon chains²¹ and (ii) the carbosilane dendrimers reach a limiting generation number more rapidly than other dendrimers due to the 3-fold branching and the short spacer unit between consecutive branching points that consists merely of three methylene units.²² However, even for G3 99% of the allylic end groups could be transformed into thioether linkages. The signal of

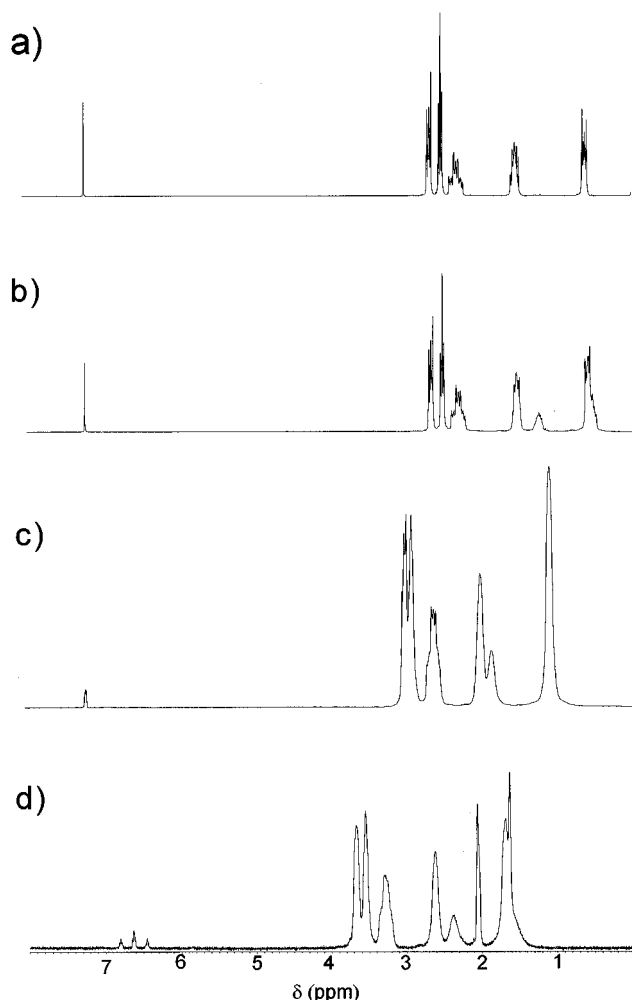


Figure 1. ^1H -NMR spectra of perfluorinated dendrimers: (a) G0-(RF6)₄; (b) G1-(RF6)₁₂; (c) G2-(RF6)₃₆; (d) G3-(RF6)₁₀₈.

residual protons of the allyl group cannot be discerned in the ^1H -NMR spectrum of G3-(RF6)₁₀₈ (Figure 1) due to the diminution of the spectra.

The dendrimers G1-(RF6)₁₂ and G2-(RF6)₃₆ are colorless liquids of increasing viscosity; G0-(RF6)₄ was obtained as a crystalline solid that melts at 23 °C. G3-(RF6)₁₀₈ is a colorless waxy solid that shows no tendency to flow even at 100 °C. The solubility of the materials in common apolar organic solvents, e.g., CHCl_3 , toluene, and hydrocarbons, decreases strongly with increasing generation number. This necessitated different workup procedures for each generation: G0-(RF6)₄ could be recrystallized from pentane/ethanol solution, and G1-(RF6)₁₂ was precipitated with ethanol from pentane solution. G2-(RF6)₃₆ and G3-(RF6)₁₀₈ are highly soluble in fluorinated solvents, e.g., C_6F_6 or perfluorohexane, but show little solubility in hydrocarbon solvents. Therefore, G2-(RF6)₃₆ and G3-(RF6)₁₀₈ could easily be purified by repeated extraction with CHCl_3 . The insolubility of the higher generations of the perfluoroalkylated dendrimers in common organic solvents is indicative of their lipophilic interior being strongly shielded by the perfluorinated segments, since highly but not quantitatively fluorinated polymers still remain soluble in many organic solvents whereas their perfluorinated analogues are soluble only in fluorocarbons.¹⁶

^1H -NMR spectra of G0-(RF6)₄, G1-(RF6)₁₂, G2-(RF6)₃₆, and G3-(RF6)₁₀₈ are shown in Figure 1. Intramolecular 5-exo-cyclization of intermediate sec-radicals, which is often observed in all-carbon systems²³ could not be

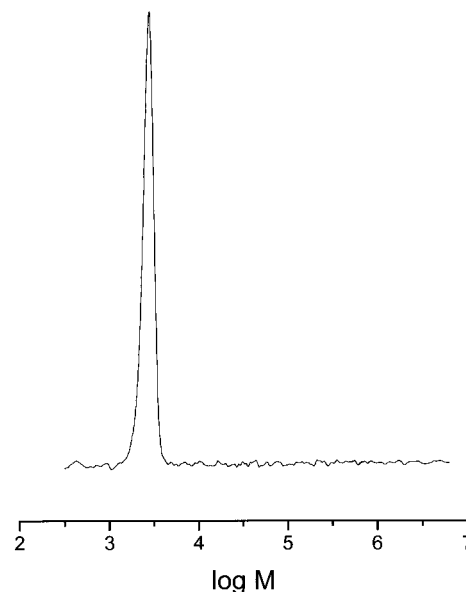


Figure 2. SEC trace of G1-(RF6)₁₂.

observed in our case. This may be assigned to the presence of the Si atom in the respective chain segment, which presumably imparts structural conditions that lower the probability of this side reaction. Furthermore, the spectra also gave no indication of Markovnikov type addition (β -addition), which has been described as a side reaction of the radical addition of ethanethiols bearing fluorinated alkyl groups.^{23a} Both reactions would become apparent in ^1H -NMR spectra by doublet signals caused by methyl groups (i.e., $\text{CH}_3\text{CHRR}'$ with R = methine group and R' = methylene group in the case of 5-exo-cyclization or R = $\text{S}(\text{CH}_2)_2\text{C}_6\text{F}_{13}$ and R' = methylene group in the case of Markovnikov type addition); however, the respective signals were not observed. In addition, 5-exo-cyclization would have led to unexpected integration ratios in the ^1H -NMR spectra, which were not observed either.

The use of free radical pathways for the functionalization of polymers is critical due to the potential occurrence of radical recombination reactions. However, the modification of polymers bearing pendant olefinic double bonds by free radical addition of mercaptans has been widely used.^{19a,24,25} In our case intermolecular side reactions of this type had to be excluded in order to maintain the low polydispersity of the dendrimers during the modification procedure. Avoidance of such reactions is an important prerequisite for the ensuing structural study. Characterization of G0-(RF6)₄ and G1-(RF6)₁₂ with respect to molecular weight distribution was carried out with SEC. In addition, the carbosilane dendrimers employed have been characterized by MALDI-TOF before.^{18b} Due to the poor solubility of G2-(RF6)₃₆ and G3-(RF6)₁₀₈ in common solvents, reasonable SEC traces of the perfluoroalkyl dendrimers could only be recorded up to G1-(RF6)₁₂. The SEC trace of G1-(RF6)₁₂ (Figure 2) evidences that high molecular weight impurities are completely absent. M_w/M_n is measured to be 1.03, which was also observed for the carbosilane dendrimers employed for the preparation of the perfluoroalkylated dendrimers. As it likewise had already been shown in previous publications,²⁶ SEC analysis based on polystyrene standards tends to underestimate the molecular weight of dendrimers grossly due to the densely packed molecular scaffold. M_n was determined to be 2700 for G1-(RF)₁₂ (expected molecular weight: 5363.64).

The excellent solubility of G2-(RF6)₃₆ and G3-(RF6)₁₀₈ in perfluorinated solvents indicates that intermolecular combination reactions leading to oligomeric species and eventual network formation did not occur during synthesis of G2-(RF6)₃₆ and if at all, only to a very limited extent during synthesis of G3-(RF6)₁₀₈.

(B) Thermal Properties. Our interest was centered on the generation-dependent thermotropic phase behavior of the flexible, lipophilic carbosilane dendrimers with perfluoroalkyl end groups, i.e., on the structural consequences of the conflict between spherically symmetrical, highly branched topology and the tendency of the perfluoroalkyl groups to align paired with their ability to phase separate from the carbosilane core. Generally, amphiphiles with lipophilic and perfluoroalkyl segments tend to self-organize into layered superstructures due to the immiscibility of perfluoroalkyl chains with alkyl groups and their stiffness, which they have in common with classical calamitic mesogens. In addition, the difference in cross section of (CF₂)_n chains compared to that of hydrocarbon chains²¹ may lead to the formation of mesophases. In the case of the linear microblock copolymers,^{13,14} the perfluorocarbon parts of the polymer are located adjacent to hydrocarbon parts of other chains, which results in a space-filling packing mode of these macromolecules. Perfluoroalkyl chains have been attached to poly(methylsiloxane) via long spacer segments using the hydrosilylation reaction,²⁷ resulting in mesophases whose transition temperatures depended on the proportion of modified siloxane units and on the length of the perfluoroalkyl side group. Polyesters with perfluoroalkyl substituents show LC phases even without the use of spacer segments, provided that the main chain flexibility is sufficient.²⁸ Recently, a study on poly(perfluoroalkyl) acrylates revealed that the mesophase structure depended on (i) the length of the perfluoroalkyl side chains, (ii) the substituents at the α -carbon of the monomeric unit and (iii) the temperature.²⁹

In general it is observed that di- and triblock molecules of the form H(CH₂)_n(CF₂)_mF and H(CH₂)_n(CF₂)_m(CH₂)_nH approximate the melting points of the resulting perfluorinated hydrocarbons for low n/m ratios and the melting points of the respective n -alkanes¹¹ for large n/m ratios. Mesophases are observed for diblock molecules of the form F(CF₂)₁₂(CH₂)_n for $4 \leq n \leq 12$.³⁰

G0-(RF6)₄ was obtained as a white powder under ambient conditions and shows a single endotherm in DSC at 23 °C, which indicates melting, i.e., isotropization ($\Delta H_m = 33.9$ kJ/mol). The compound exhibits no mesophase. The diffraction pattern is complex and supports a highly crystalline, layered structure, quite similar to what is known for the structure of perfluorinated alkanes.³¹

In contrast, G1-(RF6)₁₂ is obtained as a liquid under ambient conditions and displays intriguing thermal characteristics. A T_g as well as one phase transition at -16 °C are observed in DSC thermograms, as shown in Figure 3. The material could easily be sheared between glass slides in the temperature range between -16 °C and the glass transition temperature at -30 °C. The peak overlaying the T_g is due to an enthalpy relaxation. This can clearly be seen when higher heating rates are employed.

The enthalpy of isotropization amounts to 1.56 J/g, which is significantly lower than the isotropization enthalpy ($S_{A \rightarrow I}$) measured in the case of poly(methyl

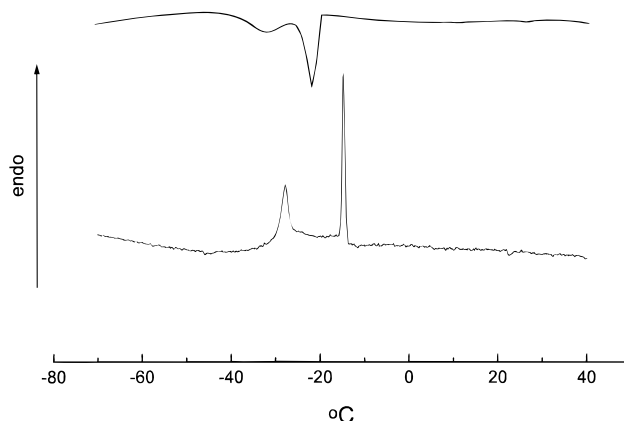


Figure 3. DSC traces of G1-(RF6)₁₂; (top) cooling scan (20 °C/min); (bottom) heating scan (3 °C/min).



Figure 4. Texture of G1-(RF6)₁₂ at -17 °C observed between crossed polarizers.

acrylate) bearing C₈F₁₇ side chains (6.5 J/g).³² The DSC trace shows a striking resemblance to the DSC trace of carbosilane dendrimers substituted with cyanobiphenyl mesogens, reported recently by our group.⁸ The mesophase exhibited by G1-(RF6)₁₂ was further characterized by polarizing microscopy (POM) and wide angle X-ray scattering (WAXS). The texture obtained by annealing the sample just below the isotropization temperature at -17 °C is displayed in Figure 4.

The fully developed texture is not specific but resembles textures of smectic A phases.³³ Similar textures have been observed for other semifluorinated polymers¹³ and fluorinated amphiphiles.³⁴ The WAXS pattern obtained from the mesophase of G1-(RF6)₁₂ is shown in Figure 5. It shows five clearly discernible reflections, three very sharp ones being located between $0^\circ < \theta < 5^\circ$ and two broad ones at $2\theta = 18.2$ and 38° , respectively. The large small angle peak translates to a d value of 26.7 Å (d_1). The location of the higher order reflections amount on the q scale to 1.97 and 2.82 times the value obtained for the first-order signal. This clearly evidences that the mesophase structure is layered. The diffraction pattern shows the layer spacing (26.7 Å) and the first two higher order reflections. The comparatively broad peak centered at $2\theta = 18.2^\circ$ is the result of the interference between C₆F₁₃ units. It represents a mean distance of 4.9 Å between the perfluorohexyl groups, which is in accordance with data for a polyacrylate bearing perfluorinated alkyl side chains.³⁵ The broad peak around $2\theta = 38^\circ$ is characteristic for the helical structure of the C₆F₁₃ units. From considerations that take into account the calculated cross section

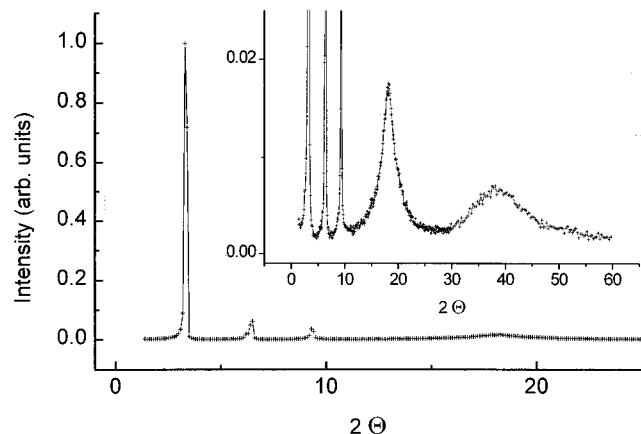


Figure 5. WAXS pattern of G1-(RF6)₁₂ at -50 °C in the range of $2\theta = 0$ –25°. Inset: wide angle region, enhanced.

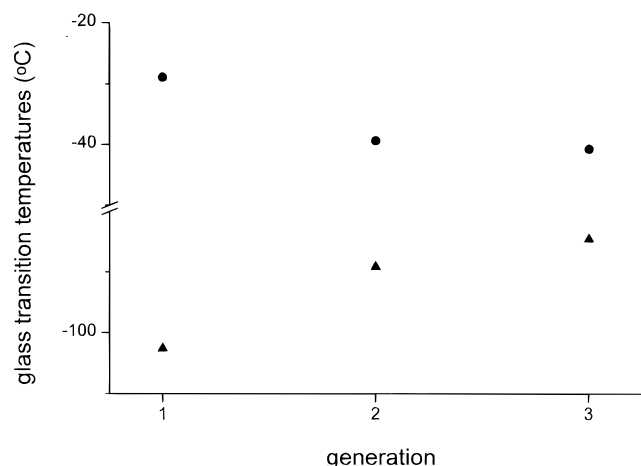


Figure 6. Glass transition temperatures of allyl-terminated (▲) and perfluorinated (●) dendrimers.

of the nonfunctionalized G1 dendrimer (15–20 Å), the length of a perfluorinated hexamethylene group (7.8 Å),¹⁴ and their mean distance in the mesophase, it was concluded that the perfluoroalkyl units interdigitate.

In contrast to G1, neither in DSC nor in POM are phase transitions discernible for the dendrimers G2-(RF6)₃₆ and G3-(RF6)₁₀₈. Glass transition temperatures were observed at -39 and -41 °C, respectively. The tendency of these materials neither to crystallize nor to exhibit a smectic mesophase was expected due to the high density of surface groups and the absence of a spacer of sufficient length that would help to decouple the stiff perfluoroalkyl groups from the dendrimer core and consequently allow them to pack into a parallel arrangement. Generally, glass transition temperatures of dendrimers are known to depend strongly on the number and polarity of the end groups.³⁶ The glass transition temperatures of the allyl-functionalized precursor molecules are observed at -103 °C (G1), -89 °C (G2), and -85 °C (G3). Clearly, modification of the dendrimer surface with groups that differ strongly in polarity or flexibility from the interior of the molecule leads to an increase in T_g , as also observed in other cases.^{8,18b,36b}

The T_g 's of the allyl-terminated and the perfluoroalkyl-functionalized dendrimers are plotted versus generation number in Figure 6.

Interestingly, only the dendrimers with allyl end groups fit into the expected relationship between molecular weight and number of end groups of dendritic

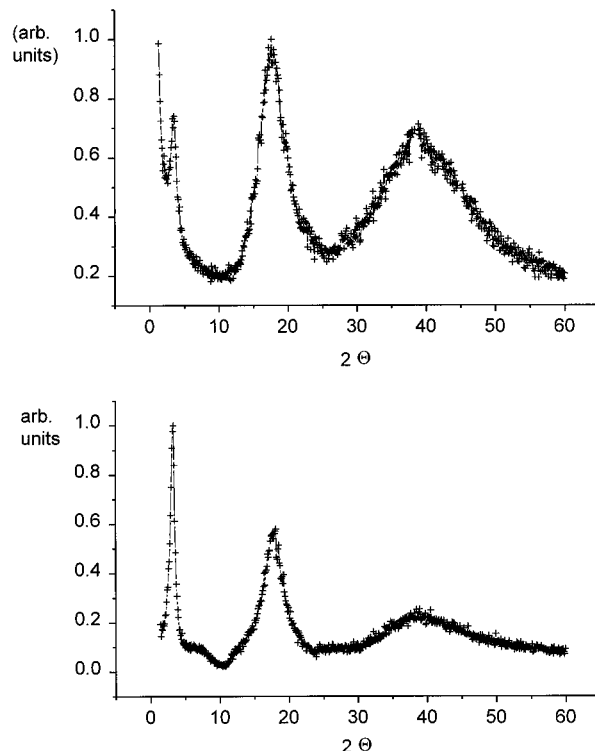


Figure 7. WAXS patterns of G2-(RF6)₃₆ at ambient temperature (top) and at -53 °C (bottom).

molecules, which predicts an increase of T_g with molecular weight.³⁶ Data available for the glass transition of smectic linear poly(siloxanes) bearing 4-oxy-(4-methoxyphenyl)benzoate side groups as mesogenic units also reveal an increase of T_g with the degree of polymerization.³⁷ The unusually high T_g of the perfluoroalkyl-substituted G1-(RF)₁₂ dendrimer can be explained by the preordering of the molecular scaffold on cooling due to the preceding formation of the mesophase, which results in a decrease in free volume and consequently restricted mobility of the inner molecular segments. However, in comparison with the larger dendrimers, we do not observe a pronounced reduction of ΔC_p (0.5 J g⁻¹ K⁻¹) at the glass transition due to the presence of the smectic structure of G1-(RF6)₁₂. In the case of side chain liquid crystalline polymers forming smectic mesoglasses a comparatively smaller ΔC_p at the glass transition is frequently observed.³⁸

In spite of their lack of any enthalpic transitions observable in DSC, G2-(RF6)₃₆ and G3-(RF6)₁₀₈ show interesting WAXS patterns in the small angle region that indicate supramolecular ordering of these materials. The X-ray diffraction patterns of G2-(RF6)₃₆ recorded at ambient temperature (liquid state) and below T_g (220 K) are shown in Figure 7.

The diffraction pattern of G2-(RF6)₃₆ at ambient temperature displays three reflections, revealing that the material is considerably less ordered than G1-(RF6)₁₂ in the liquid crystalline state. The reflection observed at ambient temperature at $2\theta = 3.4^\circ$ corresponds to a typical length of 26.0 Å. At higher angles two broader reflections are observed, one at $2\theta = 17.6^\circ$ and one at $2\theta = 39^\circ$. On cooling below T_g , the small angle peak at 3.4° gains intensity and its position shifts slightly to $2\theta = 3.3^\circ$. The correlation length now amounts to 26.8 Å. Additional scattering intensity appears as a broad shoulder at $2\theta = 6.5^\circ$, which corresponds to a correlation length of 13.6 Å. The ratio of the two correlation lengths is approximately 2, which

may indicate the presence of a layered structure, developing gradually over a broad temperature range and without pronounced heat flow in DSC. In addition, we do not observe an increase in the layer spacing in going from G1-(RF6)₁₂ to G2-(RF6)₃₆. Interestingly, the signal that reflects the correlation between the perfluorinated end groups possesses a larger half-width than in the case of G1-(RF6)₁₂ and its maximum is shifted toward slightly smaller angles ($2\theta = 17.7^\circ$). This indicates a larger mean distance between the C₆F₁₃ units and that the correlation among them is worse than in the case of the perfluorinated G1 dendrimer. As already mentioned in the case of G1-(RF6)₁₂, the broad signal located at $2\theta = 39^\circ$ originates from the helical structure of the perfluorinated end groups of the dendrimers. In summary, G2-(RF6)₃₆ probably exhibits a layered structure at low temperature. Apparently, due to the restricted mobility of the dendrimer segments, the development of the structure occurs gradually, and consequently, no enthalpic transition can be observed in DSC.

A comparison of the mesogen-substituted dendrimers with common side chain LC polymers appears interesting. In the case of side chain liquid crystalline polymers the development of smectic phases can be initiated at different parts of the chain independently. This finally leads to a situation in which the backbone is mainly restricted between the layers of the mesogens and may sometimes hop from one layer into an adjacent one due to entropic contributions to the free energy of the whole system.³⁹ In contrast, mesogen-substituted dendrimers must move as a whole in order to self-assemble into a layered superstructure. This process is kinetically considerably less favored than in the case of linear side chain polymers.

The diffraction pattern of G3-(RF6)₁₀₈ depicted in Figure 8 was recorded at 25 °C from a sample of G3-(RF6)₁₀₈, obtained from solution after slow evaporation of the solvent. It shows one large reflection at $2\theta = 2.8^\circ$ in the small angle region and additional small reflections at slightly higher angles. In the wide angle region, the diffraction pattern resembles the scattering diagrams obtained for G1-(RF6)₁₂ and G2-(RF6)₃₆.

The mean distance between the perfluorohexyl units amounts to 5.1 Å, which is comparable to the value found for G2-(RF6)₃₆ at ambient temperature. An enhanced image of the range of 2θ between 0 and 8° of the diffraction pattern furnishes evidence for the formation of a better ordered structure than observed in the diffraction pattern of G2-(RF6)₃₆. The ratio of the q values of the peaks marked by arrows is calculated to be 1: $\sqrt{3}$: $\sqrt{4}$: $\sqrt{7}$. This does not correspond to a layered structure like in the case of G2-(RF)₃₆ but may indicate the presence of a hexagonal structure. The small intensity of the higher order reflections, however, reveals that the structure is not well developed and makes it difficult to assign the type of packing with certainty. The absence of a 001 peak may further point to an arrangement of cylindrical domains on a hexagonal lattice. The 100 peak corresponds to a layer spacing of 32 Å and consequently to a closest distance between the columns in a hexagonal array of 37 Å. Additionally, a small, pronounced shoulder can be discerned at $2\theta = 2^\circ$ which might reflect the correlation of the single molecules within the columns. It corresponds to a distance of 44 Å.

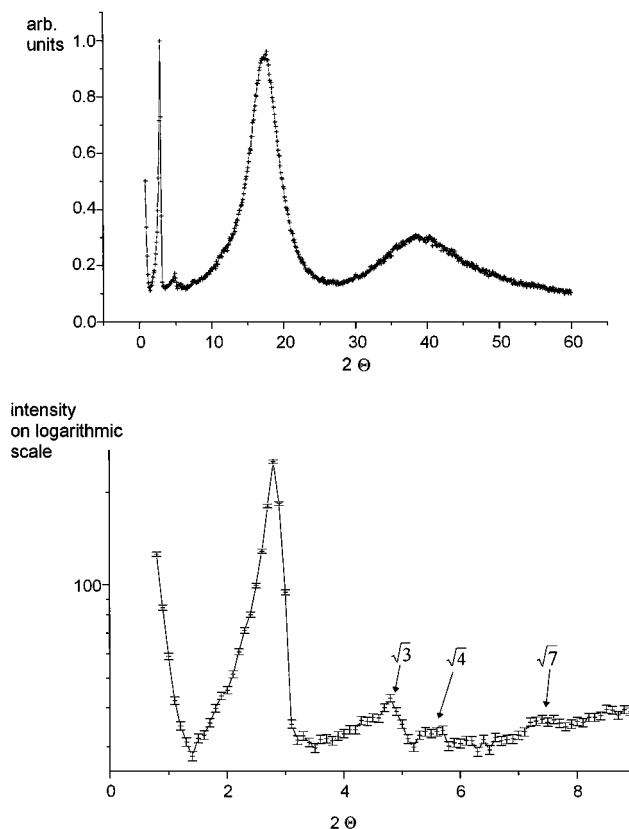


Figure 8. WAXS pattern obtained from G3-(RF6)₁₀₈ after evaporation of the solvent at ambient temperature. Bottom: enhancement in the range $2\theta = 0-9^\circ$. For clarification intensity is plotted on a logarithmic scale; error bars are included.

The X-ray diffraction patterns we obtained at 100 °C and after cooling to ambient temperature again are displayed in Figure 9.

As observed in the case of G2-(RF6)₃₆, the intensity of the small angle peak decreases considerably on heating compared to the two peaks originating from the mesogen distance and the helical structure of the perfluorinated chains. As with G2-(RF6)₃₆ no significant shift of the location of these peaks with temperature is observed. After cooling back to ambient temperature, the hexagonal structure is much less well developed than by evaporating the solvent; only the two reflections at smallest angles can be discerned in the small angle region. In summary, the following superstructure is proposed for G3-(RF6)₁₀₈ from diffraction data: The molecules organize into rows of stacked dendrimers, with the perfluorinated surface of the constituting dendrons pointing outward. A tentative sketch of that process is given in Figure 10.

These rows assemble into a hexagonal arrangement. Thus, the immiscibility of the C₆F₁₃ units with the dendritic core together with their tendency to interact by alignment results in the development of this structure.

Conclusions

Highly defined, lipophilic and flexible carbosilane dendrimers bearing a perfluorinated shell have been prepared via radical grafting of a 2-(perfluoroalkyl)ethyl mercaptan onto allyl-functionalized precursor dendrimers. The resulting materials show interesting generation-dependent thermal characteristics that cover the whole spectrum from low molecular weight organic

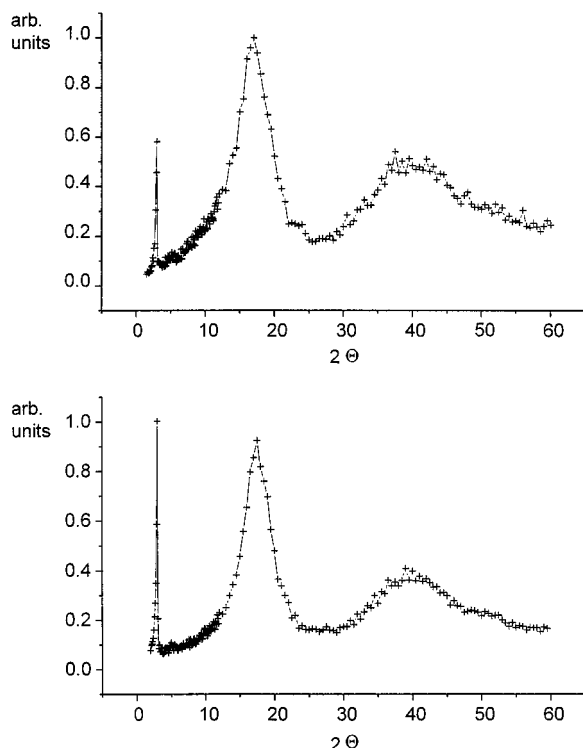


Figure 9. WAXS patterns of G3-(RF6)₁₀₈ at 100 °C (top) and after cooling back to ambient temperature (bottom).

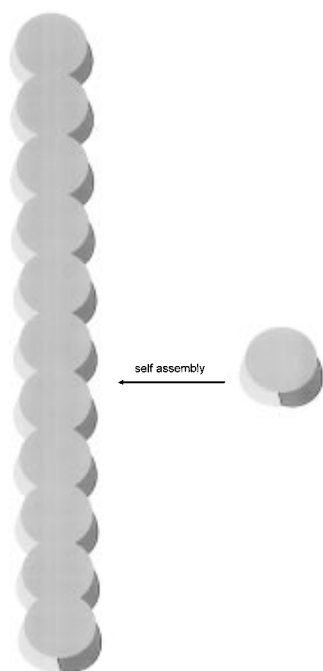


Figure 10. Proposed process of ordering of G3-(RF6)₁₀₈ (right: single dendrimer molecule, three of four dendrons visible) into a row of stacked molecules (left).

compounds, which crystallize and show simple melting behavior, to highly branched macromolecules with amphiphilic core-shell geometry developing different superstructures. We observe a transition from a smectic layered structure (G1-(RF6)₁₂) to a hexagonal arrangement of cylinders (G3-(RF6)₁₀₈). In polymers possessing hydrophobic main chains and nonionic peptide side chains, the transition from a smectic structure to hexagonally ordered cylinders can be induced, e.g., by increasing the volume of the hydrophilic part by adding water.⁴⁰ Since the volume proportion of the fluorinated

shell of the dendrimers decreases slightly from generation 1 to generation 3, the observation of hexagonally ordered columns in our case must be ascribed to the specific coupling of the C₆F₁₃ units by the dendritic scaffold. In going from G1-(RF6)₁₂ to G3-(RF6)₁₀₈ the molecule's surface becomes bent due to the increasingly dense shell. The carbosilane interior cannot deform sufficiently to allow the stiff end groups to be packed within layers.

Acknowledgment. Barbara Heck (Department of Physics) is acknowledged for invaluable assistance during the x-ray measurements.

References and Notes

- (1) Newkome, G. R.; Moorefield, C. N.; Baker, G. R.; Johnson, A. L.; Behera R. K. *Angew. Chem., Int. Ed. Engl.* **1991**, *30*, 1178.
- (2) Hawker, C. J.; Wooley, K. L.; Fréchet, J. M. J. *J. Chem. Soc., Perkin Trans. 1* **1993**, 1287–1297.
- (3) Issberner, J.; Moors R.; Vögtle, F. *Angew. Chem., Int. Ed. Engl.* **1994**, *33*, 2413.
- (4) Kim, Y. H. *J. Am. Chem. Soc.* **1992**, *114*, 4947–4948.
- (5) Bauer, S.; Fischer, H.; Ringsdorf, H. *Angew. Chem. Int. Ed. Engl.* **1993**, *32*, 1589.
- (6) Percec, V.; Chu, P.; Kawasumi, M. *Macromolecules* **1994**, *27*, 4441–4453.
- (7) Percec, V.; Chu, P.; Ungar, G.; Zhou, J. *J. Am. Chem. Soc.* **1995**, *117*, 11441–11454.
- (8) Lorenz, K.; Höltzer, D.; Stühn, B.; Mülhaupt, R.; Frey, H. *Adv. Mater.* **1996**, *8*, 414.
- (9) Frey, H.; Lorenz, K.; Mülhaupt, R. *Macromol. Symp.* **1996**, *102*, 19–26.
- (10) Höpken, J.; Möller, M. *Macromolecules* **1992**, *25*, 2482–2489 and references cited therein.
- (11) Twieg, R. J.; Rabolt, J. F. *Macromolecules* **1988**, *21*, 1806–1811.
- (12) Napoli, M. *J. Fluorine Chem.* **1996**, *79*, 59–69.
- (13) Wilson, L. M.; Griffin, A. C. *Macromolecules* **1993**, *26*, 6312–6314.
- (14) Davidson, T.; Griffin, A. C.; Wilson, L. M.; Windle, A. H. *Macromolecules* **1995**, *28*, 354–357.
- (15) (a) Percec, V.; Schlueter, D.; Kwon, Y. K.; Blackwell, J.; Möller, M.; Slangen, P. J. *Macromolecules* **1995**, *28*, 8807–8818. (b) Percec, V.; Johansson, G.; Ungar, G.; Zhou, J. *J. Am. Chem. Soc.* **1996**, *118*, 9855–9866. (c) Johansson, G.; Percec, V.; Ungar, G.; Zhou, J. P. *Macromolecules* **1996**, *29*, 646–660.
- (16) Feiring, A. E. *J. Macromol. Sci., Pure Appl. Chem.* **1994**, *A31* (11), 1657–1673.
- (17) Chapman, T. M.; Mahan, E. J. *Polym. Mater. Sci. Eng.* **1995**, *73*, 275.
- (18) (a) Van der Made, A. W.; van Leeuwen, P. W. N. M. *J. Chem. Soc., Chem Commun.* **1992**, 1400–1401. (b) Lorenz, K.; Mülhaupt, R.; Frey, H.; Rapp, U.; Mayer-Posner, F.-J. *Macromolecules* **1995**, *28*, 6657–6661.
- (19) (a) Boutevin, B.; Hervaud, Y.; Nouri, M. *Eur. Polym. J.* **1990**, *26*, 877–882. (b) Nishikubo, T.; Kameyama, A.; Sasano, M.; Sawada, M.-A. *J. Polym. Sci., Part A: Polym. Chem.* **1993**, *31*, 91–97. (c) Klemm, E.; Gorski, U. *Angew. Makromol. Chem.* **1993**, *207*, 187–193.
- (20) Masuda, Y.; Hoshi, M.; Nunokawa, Y.; Arase, A. *J. Chem. Soc., Chem Commun.* **1991**, 1444–1445.
- (21) Höpken, J.; Pugh, C.; Richtering, W.; Möller, M. *Makromol. Chem.* **1988**, *189*, 911–925.
- (22) (a) Frey, H.; Lorenz, K.; Lach, C. *Chem. Unser. Z.* **1996**, *75*, 85. (b) Lach, C.; Brizzolara, D.; Frey, H. *Macromol. Theory Simul.* **1997**, *6*, 371–380.
- (23) (a) Brace, N. O. *J. Fluorine Chem.* **1993**, *62*, 217–241. (b) Orchin, M. *J. Chem. Educ.* **1989**, *66*, 586–588. (c) Hartung, J.; Stowasser, R.; Vitt, D.; Bringmann, G. *Angew. Chem., Int. Ed. Engl.* **1996**, *35*, 108, 2820–2823.
- (24) Nakamura, H.; Takata, T.; Endo, T. *Macromolecules* **1990**, *23*, 3032–3035.
- (25) Boutevin, B.; Fleuri, E.; Parisi, J.-P.; Piétrasanta, Y. *Macromol. Chem.* **1989**, *190*, 2363–2372.
- (26) (a) Hawker, C. J.; Fréchet, J. M. J. *J. Am. Chem. Soc.* **1990**, *112*, 7638–7647. (b) Morikawa, A.; Kakimoto, M.; Imai, Y. *Macromolecules* **1992**, *25*, 3247–3253.

- (27) Beyou, E.; Babin, P.; Bennetau, B.; Dunogues, J.; Teyssie, D.; Boileau, S. *J. Polym. Sci., Part A: Polym. Chem.* **1994**, *32*, 1673–1681.
- (28) Wilson, L. M.; Griffin, A. C. *Macromolecules* **1994**, *27*, 1928–1931.
- (29) Shimizu, T.; Tanaka, Y.; Kutsumizu, S.; Yano, S. *Macromolecules* **1996**, *29*, 156–164.
- (30) Russell, T. P.; Rabolt, J. F.; Twieg, R. J.; Siemens, R. L.; Farmer, B. L. *Macromolecules* **1986**, *19*, 1135–1143.
- (31) Kimmig, M.; Steiner, R.; Strobl, G.; Stühn, B. *J. Chem. Phys.* **1993**, *99*, 8105.
- (32) Volkov, V. V.; Platé, N. A.; Takahara, A.; Kajiyama, T.; Amaya, N.; Murata, Y. *Polymer* **1992**, *33*, 1316–1320.
- (33) Gray, G. W.; Goodby, J. W. G. *Smectic Liquid Crystals, Textures and Structures*, 1st ed.; Leonard Hill: Glasgow and London, 1984.
- (34) Wilson, L. M. *Macromolecules* **1995**, *28*, 325–330.
- (35) Jariwala, C. P.; Mathias, L. J. *Macromolecules* **1993**, *26*, 5129–5136.
- (36) (a) Stutz, H. *J. Polym. Sci., Polym. Phys. Ed.* **1995**, *33*, 333.
(b) Wooley, K. L.; Hawker, C. J.; Pochan, J. M.; Fréchet, J. M. J. *Macromolecules* **1993**, *26*, 1514.
- (37) Stevens, H.; Rehage, G.; Finkelmann, H. *Macromolecules* **1984**, *17*, 851.
- (38) Finkelmann, H. In *Liquid Crystallinity in Polymers*; Ciferri, A., Ed.; VCH: New York, Weinheim, Cambridge, 1994; p 324.
- (39) Warner, M. In *Side Chain Liquid Crystal Polymers*; McArdle, C. B., Ed.; Glasgow, London, 1989; pp 18–21.
- (40) (a) Gallot, B.; Marchin, B. *Liq. Cryst.* **1989**, *5*, 1719–1727.
(b) Gallot, B. *Mol. Cryst. Liq. Cryst.* **1991**, *203*, 137–148.

MA970282W